

## ■ Porphyrins

## Synthesis and Characterization of New Conjugated Fluorenyl-Porphyrin Dendrimers for Optics

Dandan Yao,<sup>[a, b]</sup> Xu Zhang,<sup>[a, b]</sup> Olivier Mongin,<sup>[a]</sup> Frédéric Paul,<sup>[a]</sup> and Christine O. Paul-Roth\*<sup>[a, b]</sup>

Dedicated to Professor Jean-Marie Lehn on the occasion of the 50th anniversary of his laboratory: thank you for having transmitted to us the passion of creating beautiful architectures

**Abstract:** A new family of conjugated *meso*-tetraphenylporphyrin-based dendrimers with four (TPP1, TPP2), eight (TPP3, TPP4, TPP5) and up to sixteen (TPP6) fluorenyl groups has been synthesized and fully characterized. These tetraphenylporphyrin-cored dendrimers present peripheral alkynyl  $\pi$ -conjugated dendrons with fluorenyl termini. The *meso*-aryl rings of these porphyrins are functionalized either

in *para*- (TPP1, TPP2, and TPP3) or *meta*-positions (TPP4, TPP5, and TPP6). Their detailed luminescence properties are discussed in reference to two porphyrins lacking fluorenyl dendrons (TPP-H<sub>1,2,3</sub> and TPP-H<sub>4,5,6</sub>). A strong dependence of their luminescence quantum yield and lifetime on their structures is stated, their nonlinear optical properties were also discussed.

## Introduction

Porphyrins are well known as light absorbers in photosynthesis. For instance, chlorophyll uses very elaborate light-harvesting systems to capture sunlight and funnel this energy to the reaction center through rapid and efficient energy transfer processes.<sup>[1]</sup> Whereas these remarkable properties have fostered a great interest in better understanding photophysical properties of porphyrins, chemists have now designed a large library of varied synthetic porphyrins for widely different applications, such as for instance light-emitting diodes,<sup>[2]</sup> artificial photosynthetic systems,<sup>[3]</sup> and organic frameworks.<sup>[4]</sup> For all these applications and many others, enhancing the light absorption of porphyrins or maximizing their emission is often central to the development of active devices.

In this respect, many porphyrin-based dendrimers have been synthesized these last decades.<sup>[5a,b]</sup> Their light-harvesting properties could be optimized by connecting highly absorbing dendrons to the porphyrin core, the former acting as energy donors to the second, overall behaving like an antenna system.<sup>[5c,d]</sup> In particular, some porphyrins bearing pendent linear oligofluorene arms have been reported in this context.<sup>[6]</sup> For

such molecular assemblies, Fréchet<sup>[7]</sup> demonstrated that the antenna effect was facilitated in dendritic architectures versus linear ones. The synthesis of systems with modified fluorenyl units for light-harvesting based on biphotonic processes was also reported.<sup>[8]</sup> More recently, hyperbranched polymers containing porphyrin with fluorenyl arms have also been synthesized for light harvesting,<sup>[9]</sup> whereas the group of Okada and Kozaki, investigated the use of series of multi-porphyrin arrays in conjugated networks as light-harvesting antenna.<sup>[10]</sup>

In this field, we also have recently reported efficient light-harvesting systems in which 5,10,15,20-tetraphenylporphyrin (TPP) was linked, through ether bridges, to four, eight, and sixteen fluorenyl donor moieties.<sup>[11a-c]</sup> We now wondered about the possibility of obtaining more efficient light-harvesting systems by preserving some  $\pi$ -overlap between the peripheral arms and the central core.<sup>[11d]</sup> Indeed, porphyrin-based dendrimers containing  $\pi$ -conjugated dendrons are expected to present better energy transfer properties than systems for which  $\pi$ -conjugation is completely disrupted, as indicated for instance by the work of Burn and Samuel on porphyrin dendrimers with stilbene dendrons.<sup>[12]</sup>

From a synthetic point of view, the *meso*-phenyl units of the TPP core molecule provide two positions that are easy to functionalize (*para* and *meta*). Therefore, we have targeted six new porphyrin-based dendrimers featuring 2-fluorene-containing dendrons with extended  $\pi$ -manifolds on these positions (Figure 1) to study their optical properties (absorption and emission). Such systems presenting an increasing number of terminal fluorenyl units in the peripheral dendrons, going from 4 to 8 to 16, will bring information about the importance of the number of fluorophores in the peripheral antennas. Furthermore, the various systems investigated can be categorized

[a] Dr. D. Yao, X. Zhang, Dr. O. Mongin, Dr. F. Paul, Dr. C. O. Paul-Roth  
Institut des Sciences Chimiques de Rennes (ISCR)-UMR CNRS 6226  
Université de Rennes 1, 35042 Rennes Cedex (France)  
E-mail: christine.paul@univ-rennes1.fr

[b] Dr. D. Yao, X. Zhang, Dr. C. O. Paul-Roth  
Institut National des Sciences Appliquées (INSA)  
Université Européenne de Bretagne, 35043 Rennes Cedex (France)

Supporting information for this article can be found under <http://dx.doi.org/10.1002/chem.201504617>, containing <sup>1</sup>H NMR and <sup>13</sup>C NMR spectra and mass spectra of all new compounds.

into *para*-substituted (**TPP1**, **TPP2**, and **TPP3**) and *meta*-substituted (**TPP4**, **TPP5**, and **TPP6**) systems. Indeed, given that the conjugation between the porphyrin core and the unsaturated dendrons should be more effective in the *para*-functionalized systems than in the *meta* ones, comparison between the photophysical properties of these two series should provide some insight about the importance of such a structural feature for the light-harvesting effect. Note also that dendrimers **TPP1** and **TPP2** (**TPP4** and **TPP5**, respectively) have nearly identical structures, except that **TPP2** (**TPP5**) has *n*-butyl substituents on the fluorenyl group. By comparison, **TPP3** and **TPP6** can be envisioned as constituting members of a later generation in the perspective of expanding the dendritic structure, whereas the two synthetic precursors of these series of molecules (**TPP-H<sub>1,2,3</sub>** and **TPP-H<sub>4,5,6</sub>**) can be used to model the optical properties of the central core of each family in the absence of peripheral dendrons.

## Results and Discussion

### Synthesis

So far, dendritic porphyrins have been synthesized essentially through two approaches, each possessing their own drawbacks.<sup>[5a,b]</sup> In the so-called “divergent” approach, the dendritic antennas of the porphyrin are gradually constructed from the porphyrin core, but unavoidable structural defects are often generated in the latest generations due to the increasing number of identical reactions to be performed in parallel. As a result, purification becomes a serious issue to isolate the largest dendrimers with a perfect structural control. In contrast, with the alternative “parallel” approach, phenylaldehyde-based dendrons are first built and the porphyrin cores are eventually assembled in the last step to obtain the desired dendrimer. Although this approach simplifies the purification steps, it is often plagued by very low yields, mostly because of the inherently low yield of the last step. In this work, both approaches were tested to prepare the targeted TPP-cored dendrimers.

At first, two divergent approaches were considered to synthesize **TPP4**, the first target of the *meta*-substituted series (Scheme 1). More precisely, two different routes, (I) and (II), were tested to access this target: either starting from the (I) octabromo-porphyrin (**8BrTPP**) and eight equivalents of alkynyl-fluorene (**1**) or (II) from the alkynyl-porphyrin (**TPP-H<sub>4,5,6</sub>**) and eight equivalents of bromofluorene. Triple bonds were introduced each time by Sonogashira couplings<sup>[13]</sup> and deprotection of the trimethylsilyl (TMS) groups was achieved using K<sub>2</sub>CO<sub>3</sub> in mixed MeOH/CH<sub>2</sub>Cl<sub>2</sub> solutions. In each case, a mixture of porphyrins was obtained in which **TPP4** could not be detected by TLC (thin layer chromatography).

We believe that this result was due to the weak solubility of this particular porphyrin, which was subsequently isolated by following a convergent approach (Scheme 2). Nevertheless, our new model porphyrin for the *meta*-family (**TPP-H<sub>4,5,6</sub>**) was successfully isolated during these trials (Scheme 3).

We next attempted to isolate **TPP4** by a convergent approach from the corresponding aldehyde (compound **5**).

During the synthesis of this aldehyde **5** (Scheme 2), we observed that the aldehyde function could react with the fluorene group under Sonogashira coupling conditions. So, protection of this aldehyde was achieved first using ethane-1,2-diol in toluene and 4-methylbenzenesulfonic acid (TsOH) as a catalyst, whereas deprotection was performed using a mixture of aqueous HCl (10% in water) and THF.<sup>[14]</sup> The desired aldehyde **5** was obtained in 56% yield by this means (Scheme 2) affording the desired **TPP4** in 2% yield after the porphyrin synthesis following an Adler–Longo protocol (Scheme 5).

Similarly for the synthesis of aldehyde dendron **3** (Scheme 2), we observed that the aldehyde function could react with the non-substituted fluorene group under Sonogashira coupling conditions. So, protection of this aldehyde followed by deprotection was necessary to obtain aldehyde **3** in 48% yield. Except for the aldehydes **3** and **5**, which require preliminary protection of the aldehyde group (Scheme 2), the other (*n*-butyl-substituted) fluorenyl-containing aldehydes were obtained directly. In more detail, aldehydes **4**, **6**, **8**, and **9** were obtained in good yields (76, 80, 66, and 58%, respectively) by using Sonogashira coupling protocols, from intermediates **2** and **7**, previously synthesized in our group (Scheme 4).<sup>[15]</sup>

In parallel, a similar series of steps using the aldehyde **6** with a fluorene group presenting *n*-butyl chains at the 9-position allowed to isolate the *n*-butyl analogue of **TPP4** (**TPP5**) in 18% yield (Scheme 5). In this case again, protection of the aldehyde before the Sonogashira coupling was not required.

These initial trials prompted us to use a similar “convergent” approach to isolate all other targeted porphyrin derivatives from the corresponding aldehydes (Scheme 5). Given that nowadays, apart from the Adler–Longo<sup>[16]</sup> method, the Lindsey<sup>[17]</sup> method is also widely used for porphyrin synthesis, we have decided to test the latter in some cases. However, we did not isolate any product when this reaction protocol was attempted to obtain **TPP2** or **TPP5**; only black tars and polymers were isolated in those cases. Subsequently to these trials, Adler–Longo conditions were always utilized to synthesize the targeted porphyrins. The desired porphyrins were successfully isolated each time, but the yields were variable (Scheme 5). We believe that these changes result from the different solubilities in the reaction medium of various aldehydes and porphyrins. For example, the non-substituted aldehyde **5**, used for **TPP4** synthesis, shows a very weak solubility in propionic acid, even at high temperature. Furthermore, the low solubility of the final porphyrins was also certainly an issue for purification. Insoluble **TPP4** was therefore absorbed on silica gel, on the top of the column, allowing elimination of all byproducts and polymers by washing several times with CH<sub>2</sub>Cl<sub>2</sub>. Eventually, the pure product **TPP4** was only partly recovered from silica by heating CH<sub>2</sub>Cl<sub>2</sub> at reflux in a Soxhlet extractor. Consequently, the final yield for **TPP4** only reached 2% from the corresponding aldehyde **5**.

Similar purification conditions were also used for **TPP1**, which allowed us to obtain a significantly better yield (17%) for that reaction. In contrast, the derivatives presenting butyl chains on the fluorenyl groups, such as **TPP2** or **TPP5**, exhibit-

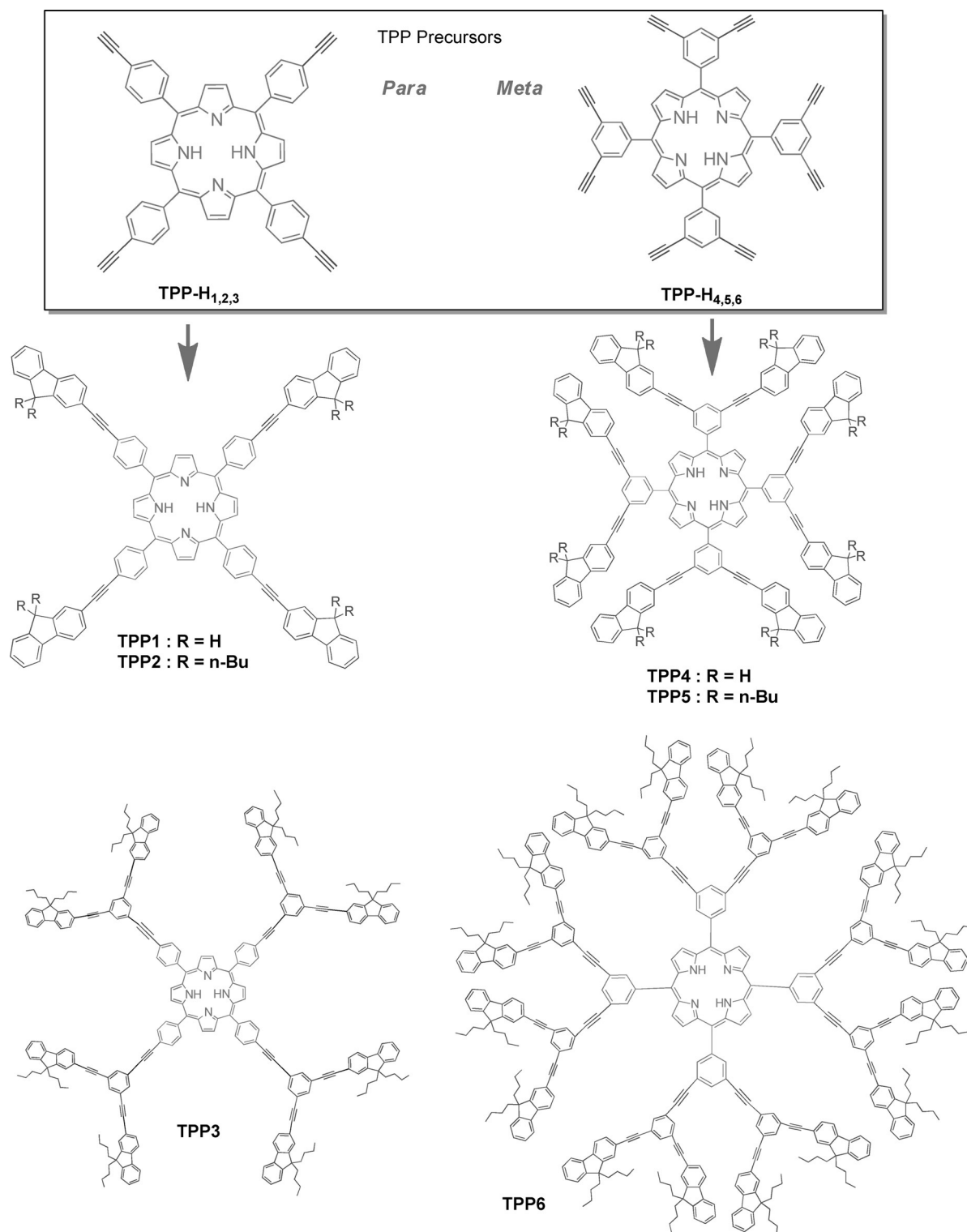
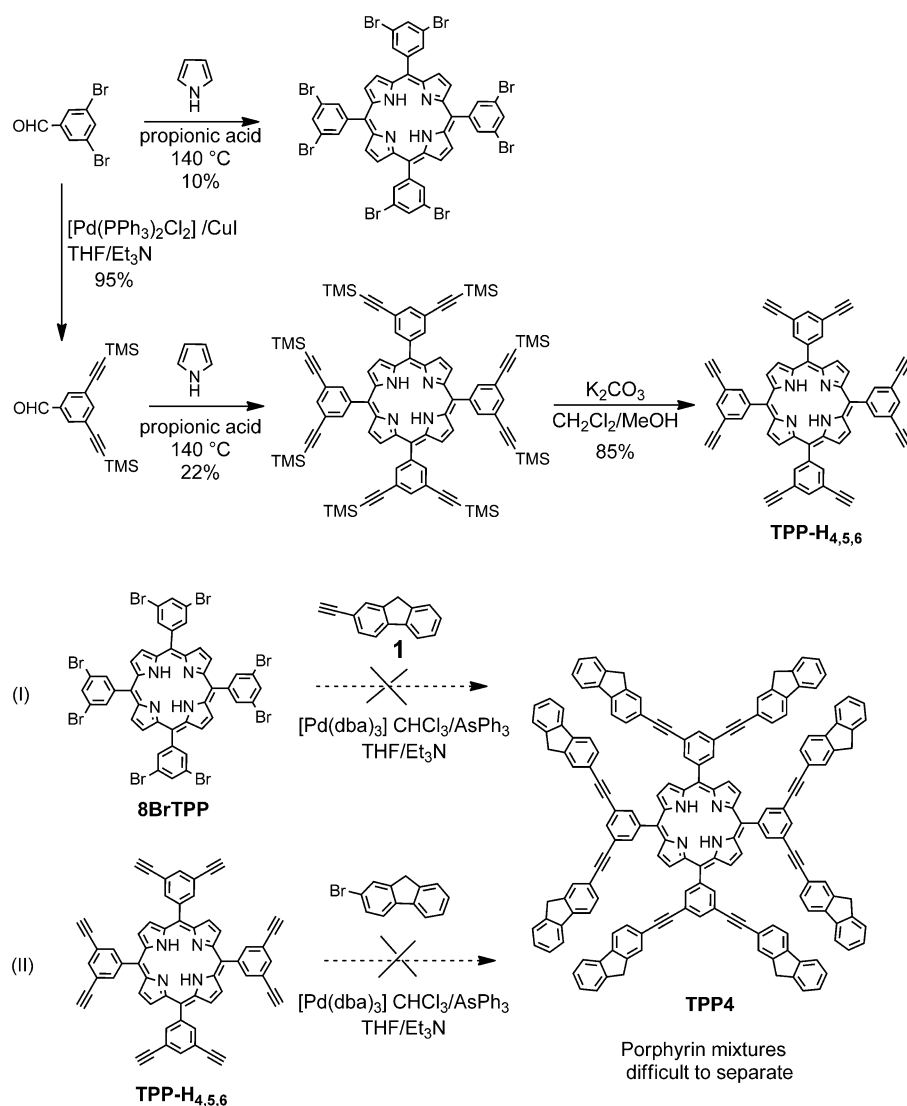


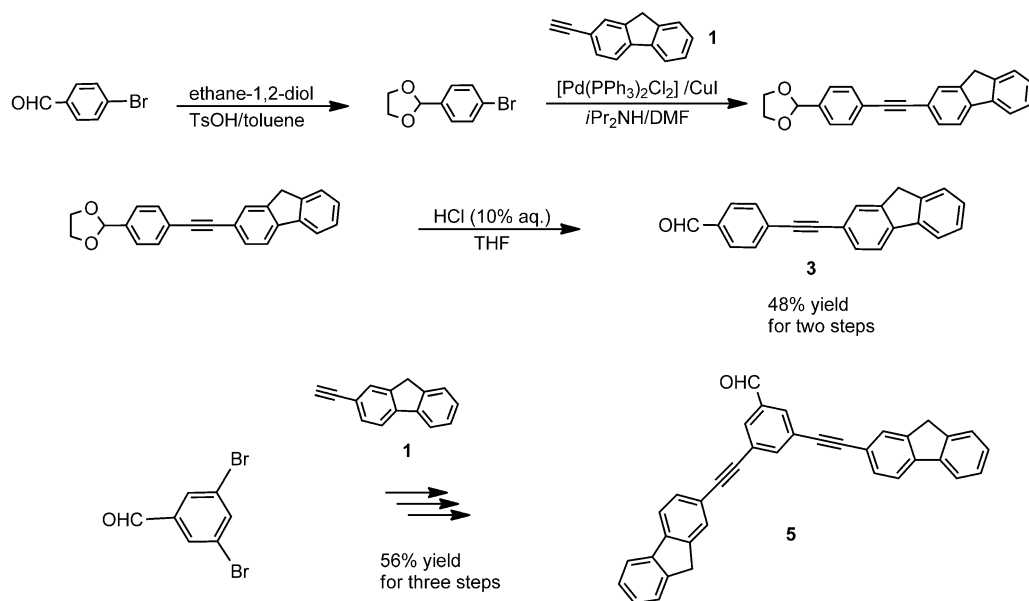
Figure 1. Molecular structures of TPP-cored porphyrin dendrimers TPP1–TPP6 and their reference.

ed a good solubility in common organic solvent and their purification could be easily achieved by classical chromatography. As a result, the overall yield for these two compounds rose to 28% and 18%, respectively. For these reasons, synthesis of the unsubstituted fluorenyl analogues of the  $\pi$ -extended porphyrins **TPP3** and **TPP6** was not attempted. The latter derivatives

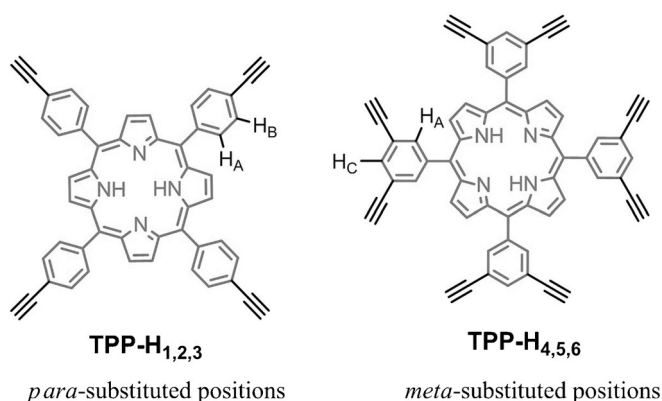
were prepared from the *n*-butyl substituted aldehydes **8** and **9** in propionic acid at 140 °C for 5.5 h, in 22 and 13% yield, respectively (Scheme 5). All these porphyrin-based dendrimers were further purified by recrystallization in distilled solutions of CHCl<sub>3</sub> and MeOH.



Scheme 1. Synthesis of 8BrTPP and TPP-H<sub>4,5,6</sub> and the two divergent routes (I) and (II) initially tested to isolate TPP4.



Scheme 2. Synthesis of the fluorenyl-containing aldehydes **3** and **5**.



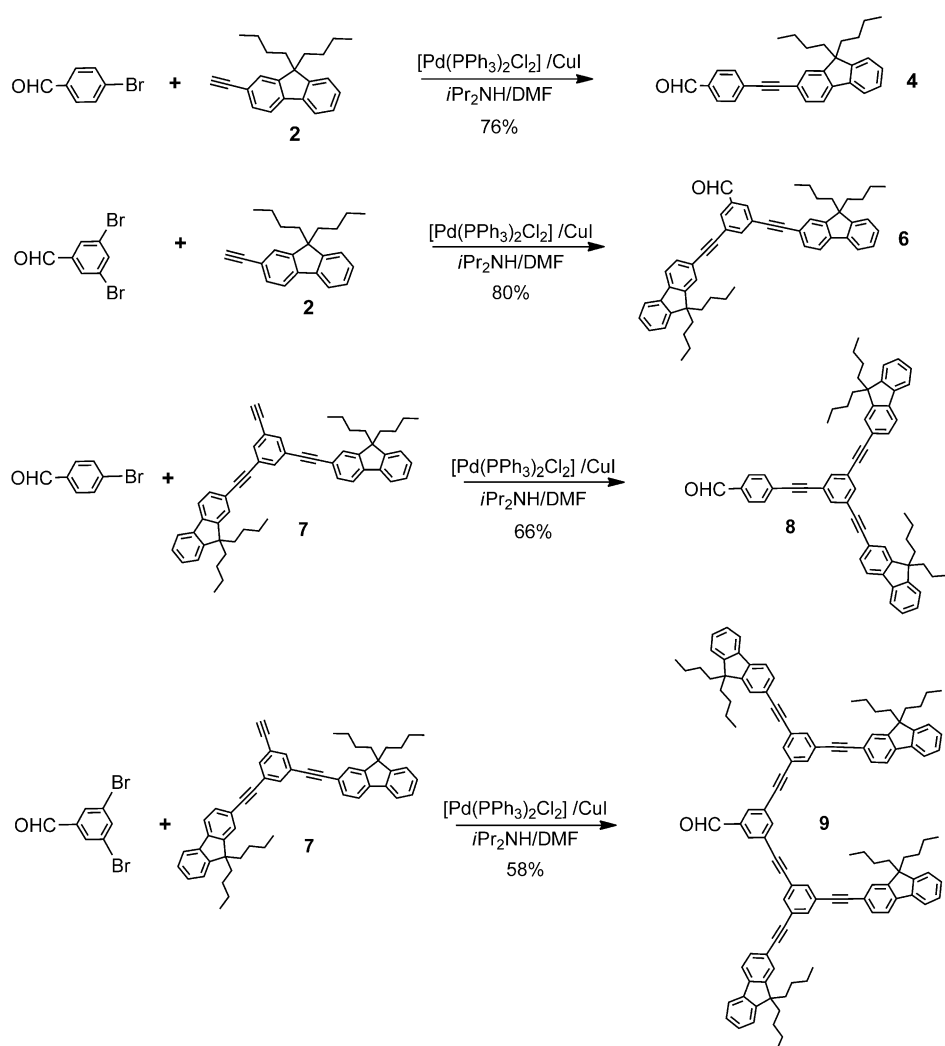
**Scheme 3.** Reference porphyrins TPP-H<sub>1,2,3</sub> and TPP-H<sub>4,5,6</sub> with hydrogen atom labeling for the *meso*-phenyl groups.

Note that another approach was also tested to obtain the extended aldehyde **8** (Scheme 6), presented before in Scheme 4. This second synthesis, starting from commercial *para*-bromobenzaldehyde, went through the intermediacy of the bis-ethynyl aldehyde derivative **12**, which was obtained

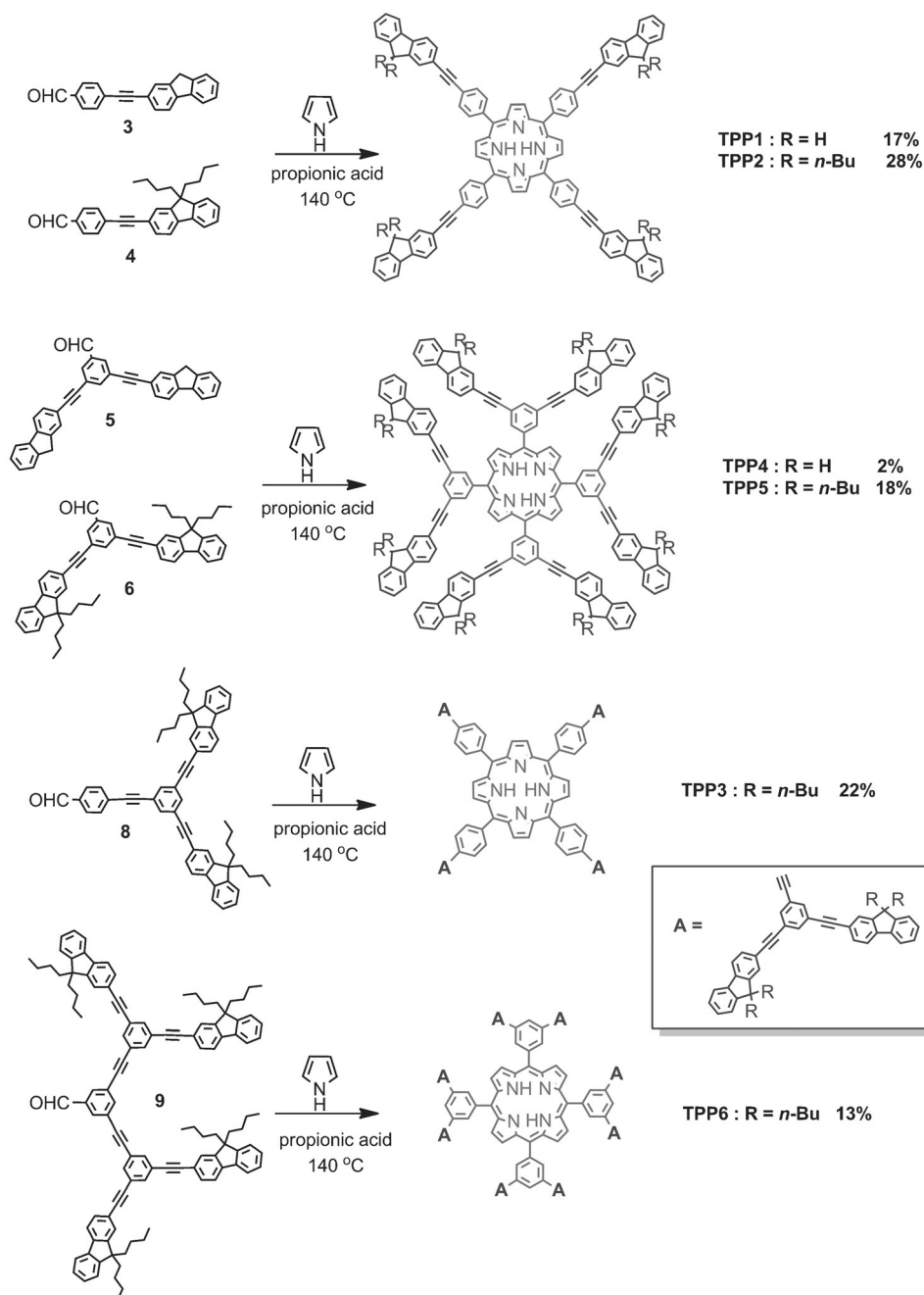
after desilylation of the aldehyde obtained subsequently to the coupling of **11** with **10**. Compound **10** was obtained in one step and good yields from the commercial 1,3,5-tribromobenzene. Whereas **10** (88%) and the aldehyde intermediates **11** (59%) and **12** (53%) were isolated in fair to good yields, the last step leading to **8** was not quantitative (aldehyde **12** might react with itself in base solution at high temperature, 75–95 °C), and only a small quantity of this new compound **8** was collected. This definitively prompted us to adopt the synthesis depicted in Scheme 4 to prepare these required aldehyde intermediates.

### <sup>1</sup>H NMR studies

As previously mentioned, the compounds TPP-H<sub>1,2,3</sub> and TPP-H<sub>4,5,6</sub> (Scheme 3) will be used as model compounds to study the properties of the *para*- (TPP1–TPP3) and *meta*-substituted (TPP4–TPP6) derivatives, respectively (Figure 1), and we would like to discuss the influence of these positions on the spectroscopic properties. The first compound, TPP-H<sub>1,2,3</sub> is a known compound that has been obtained following a reported syn-



**Scheme 4.** Synthesis of the *n*-butyl-substituted fluorenyl-containing aldehydes **4**, **6**, **8**, and **9**.



**Scheme 5.** Synthesis of porphyrin-based dendrimers by an Adler-Longo protocol from the corresponding aldehydes.

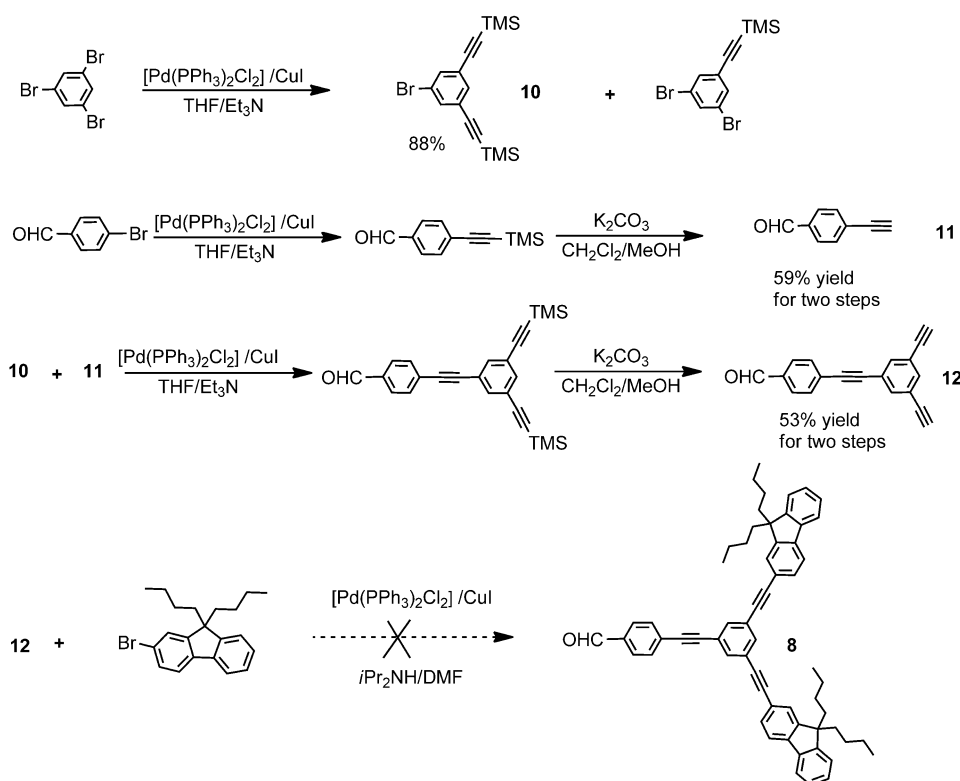
thesis,<sup>[18]</sup> whereas the second one, **TPP-H<sub>4,5,6</sub>**, was isolated as described in Scheme 1.

### <sup>1</sup>H NMR spectra of the precursor aldehydes

The signals in the <sup>1</sup>H NMR spectra of the aldehydes **3**, **4**, **5**, **6**, **8**, and **9** that constitute convenient models for the dendrons of the porphyrin-based dendrimers can appear in three distinct and characteristic spectral ranges: 1) One aldehyde proton (–CHO) near  $\delta=10$  ppm; 2) Several phenyl and fluorenyl protons in the aromatic ( $\delta=7$ –8 ppm) range, 3) Two 9-H protons

near  $\delta=4$  ppm or four groups of *n*-butyl protons in the aliphatic ( $\delta=0.5$ –2 ppm) range.

This is apparent on the spectra of the aldehydes **5** and **6** as examples (Figure 2); the fluorenyl groups of **5** being without *n*-butyl substituents and those of **6** with *n*-butyl substituents. The single peak at about  $\delta=10$  ppm corresponds to the aldehyde proton, whereas protons around  $\delta=7$ –8 ppm can confidently be assigned to the aromatic moieties. Finally, butyl protons, including four groups of protons in *n*-butyl around  $\delta=0$ –2 ppm for **5** or 9-H protons around  $\delta=4$  ppm for **6**, are diagnostic of the fluorenyl functionalization.



Scheme 6. Synthesis of modified aldehydes **11**, **12**, and the synthetic attempt to isolate the extended aldehyde **8**.

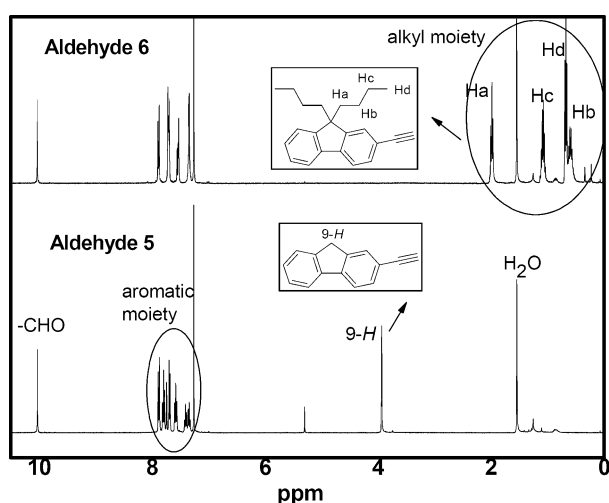


Figure 2. Detailed 400 MHz  $^1\text{H}$  NMR spectra of the precursors **5** and **6** in  $\text{CDCl}_3$ .

### $^1\text{H}$ NMR spectra of the dendrimers TPP1–6

As expected, in the final porphyrin derivatives, the aldehyde proton disappears and additional signals, diagnostic of the tetraphenylporphyrin ring, appear with the correct intensities. Thus, for the *para*-substituted (TPP1, TPP2, and TPP3) and *meta*-substituted porphyrins (TPP4, TPP5, and TPP6), one new signal corresponding to two protons is observed around  $\delta = -2.7$  ppm. This signal belongs to the nitrogen atoms in the

heart of the porphyrin located inside the shielding cone of the TPP ring. Then, a new singlet, at around  $\delta = 9$  ppm, corresponding to eight protons is also observed in each case. The latter is assigned to the  $\beta$ -pyrrolic protons that are located outside the shielding cone. Note that the observation of a unique singlet for these protons is diagnostic of a symmetrically substituted porphyrin ring. There is a small shift to the lower field for the  $\beta$ -pyrrolic protons in *meta*-substituted TPP-style porphyrin series compared with that of the *para*-substituted ones (Figure 3). Finally, numerous signals also appear in the region between  $\delta = 7.2$  and 8.5 ppm, which correspond to aromatic protons of the fluorenyl and phenyl of the dendrons, but also to the protons of the *meso* aryl groups. For the latter, only a small difference in shift is observed regardless of the compound considered. Thus,  $\text{H}_\text{A}$  and  $\text{H}_\text{B}$  for *para*-substituted porphyrins are located at  $\delta = 8.2$  and 8.0 ppm, whereas  $\text{H}_\text{A}$  and  $\text{H}_\text{C}$  for *meta*-substituted ones are located around  $\delta = 8.4$  and 8.2 ppm (Figure 3). Finally, the 9-H fluorenyl protons of TPP1 and TPP4 are observed at  $\delta = 4.2$  ppm, whereas the *n*-butyl protons of TPP2, TPP3, TPP5, and TPP6 are observed between  $\delta = 2.1$  and 0.6 ppm. The butyl groups on the fluorenyl ligands give rise to a set of four broad signals with characteristic shifts.<sup>[19]</sup>

### Absorption and emission properties of TPP1–TPP6

UV-visible absorption and emission measurements were performed for the reference porphyrins TPP, TPP-H<sub>1,2,3</sub>, TPP-H<sub>4,5,6</sub>,

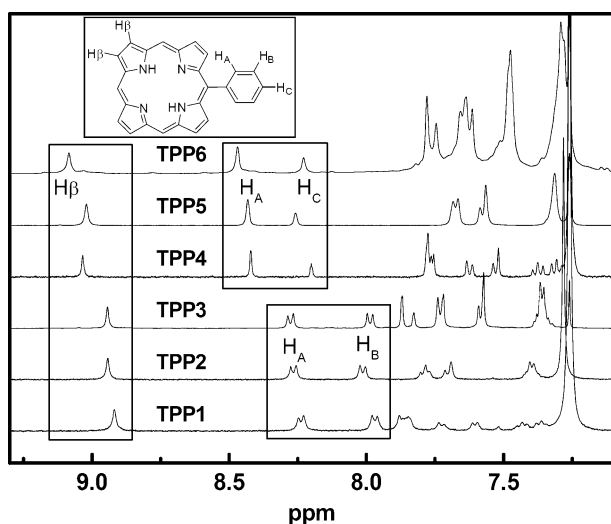


**Figure 3.** Aromatic region of the 400 MHz  $^1\text{H}$  NMR spectra of the porphyrin-based dendrimers **TPP1**, **TPP2**, and **TPP3** versus **TPP4**, **TPP5**, and **TPP6** in  $\text{CDCl}_3$ .

and for porphyrin-based dendrimers **TPP1**–**TPP6** in solution at room temperature, respectively (Table 1; Figures 4–6).

The absorption spectra of **TPP1**–**TPP6** (Figure 5 and 6) are typical for porphyrins: an intense Soret band between 425 and 428 nm, and four weaker Q-bands,  $\text{Qy}(1,0)$ ,  $\text{Qy}(0,0)$ ,  $\text{Qx}(1,0)$ , and  $\text{Qx}(0,0)$  around 518, 554, 590, and 648 nm, respectively.

All these dendrimers show a strong additional band at 324–330 nm that corresponds to the absorption of the conjugated fluorenyl dendron, as observed for compounds 1–9. In contrast, the absorption at these wavelength is, as expected, very weak for the reference compounds **TPP-H**<sub>1,2,3</sub>, **TPP-H**<sub>4,5,6</sub> and for the tetraphenylporphyrin (**TPP**) parent molecule lacking such fluorenyl groups. The main differences between these reference compounds appear on their emission spectra. Thus, for **TPP-H**<sub>4,5,6</sub>, the relative intensities of the  $\text{Q}(0,1)$  emission bands increases relative to the  $\text{Q}(0,0)$  compared with those of the two other compounds (Figure 4).<sup>[12c]</sup>

Table 1. Photophysical properties of the dendrimers <b>TPP1</b> – <b>TPP6</b> in dilute solutions at 298 K.				
dendron	Absorption <sup>[a]</sup> [nm]	Emission <sup>[a]</sup> [nm]		
		porphyrin: Soret band, Q bands	Q (0,0)	Q (0,1)
<b>TPP1</b>	320	426 518, 554, 592, 650	656	722
<b>TPP2</b>	324	426 518, 555, 592, 650	657	722
<b>TPP3</b>	330	425 520, 555, 592, 650	655	721
<b>TPP4</b>	324	428 517, 552, 589, 646	651	718
<b>TPP5</b>	326	426 517, 552, 589, 646	650	718
<b>TPP6</b>	327	426 517, 552, 590, 646	651	716

[a] Measurements in distilled  $\text{CH}_2\text{Cl}_2$  with the UV/Vis absorption region from 200 to 800 nm and emission region from 300 to 800 nm.

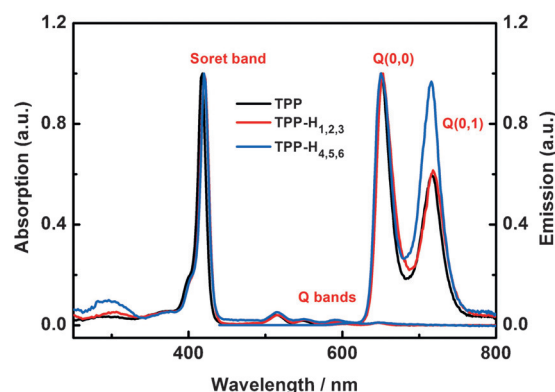


**Figure 4.** Normalized absorption and emission spectra of reference porphyrins **TPP**, **TPP-H**<sub>1,2,3</sub> and **TPP-H**<sub>4,5,6</sub>.

Figure 5 shows the normalized absorption and emission spectra of *para*-substituted **TPP**-style porphyrins **TPP1**, **TPP2**, and **TPP3** compared with the normalized absorption and emission spectra of the reference porphyrin **TPP-H**<sub>1,2,3</sub>. Relatively strong absorptions around 300 nm are observed for dendrimers possessing terminal fluorenyls in conjugated position with the porphyrin core. By normalizing the intensity of Soret band around 426 nm on the absorption spectra and the  $\text{Q}(0,0)$  emission peak around 650 nm for the emission spectra, no obvious changes are observed between the two generations except that the fluorenyl-based absorption near 300 nm is twice as strong for **TPP3**, in line with the increasing number of fluorenyl ligands in the latter compound. The similar emission spectra suggest that the shape of the porphyrin ring does not deviate significantly from planarity in the *para*-functionalized **TPP** series with change in dendrimer generation.<sup>[11c]</sup> The absence of significant modifications of the position of the bands relative to the porphyrin rings in both absorption and emission spectra also suggests that their conjugation with the fluorenyl dendrons is rather weak. However, we can notice that the intensity of Soret bands of dendrimer products, meaning the extinction coefficients ( $\epsilon$  varying from  $566 \times 10^3 \text{ m}^{-1} \text{ cm}^{-1}$  for **TPP6** to  $806 \times 10^3 \text{ m}^{-1} \text{ cm}^{-1}$  for **TPP3**) are clearly larger compared with **TPP** or **TPP-H**<sub>1,2,3</sub> (around  $440 \times 10^3 \text{ m}^{-1} \text{ cm}^{-1}$ ). This stronger transition suggests the existence of some conjugation between fluorenyl groups and the central porphyrin core. Note also that the spectrum of **TPP2** (with *n*-butyl chains on the fluorenyl ligand) presents almost no difference to that of **TPP1**.

Figure 6 shows the normalized absorption and emission spectra of *meta*-substituted **TPP**-style porphyrins: **TPP4**, **TPP5**, and **TPP6** compared to the reference porphyrin **TPP-H**<sub>4,5,6</sub>. Each generation of the *meta*-substituted porphyrin dendrimers has a larger number of terminal fluorenyl groups than the *para* ones in its peripheral dendrons. Without surprise, the intensity of the absorption near 300 nm relative to the Soret band is therefore stronger for the *meta*-functionalized series for a given dendrimer generation. Note however that the intensity of this band for **TPP4** or **TPP5** is slightly lower than for that of **TPP3**, whereas these three compounds possess eight fluorenyl groups. This slightly stronger transition suggests the existence

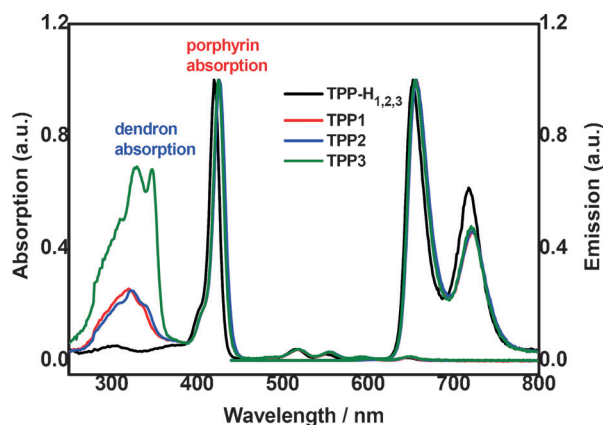


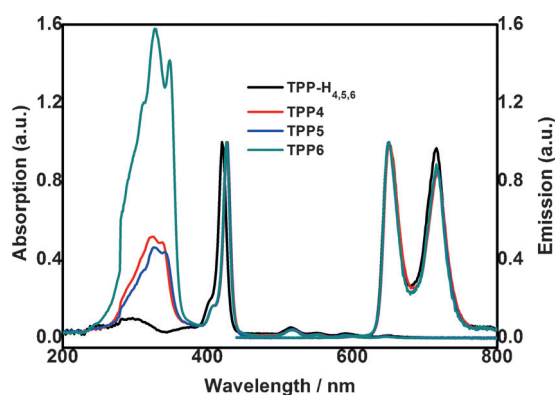
**Figure 5.** Normalized absorption and emission spectra of *para*-substituted porphyrins-based dendrimers **TPP1**, **TPP2**, **TPP3** and the corresponding reference compound **TPP-H<sub>1,2,3</sub>**.

of some conjugation between *para*-connected fluorenyl groups and the central porphyrin core. In the same line, a slight bathochromic shift (6 nm) of this particular absorption is also stated for **TPP3** relative to **TPP4** or **TPP5**. Then, among the *meta*-functional derivatives, **TPP6** features the strongest absorption in line with the larger number of fluorenyl groups in the peripheral dendrons. Apart from that, the rest of their spectra, which correspond to transitions specific to the porphyrin chromophore, are nearly identical, likewise to their emission spectra. This indicates that the conjugation between porphyrin and dendrons is very weak in the *meta* series. Again, this can also be taken as an indication that no specific deformation of the porphyrin plane is induced by the various dendrons when progressing from **TPP4** to **TPP6**.

### Energy transfer from fluorenyl unit to porphyrin core

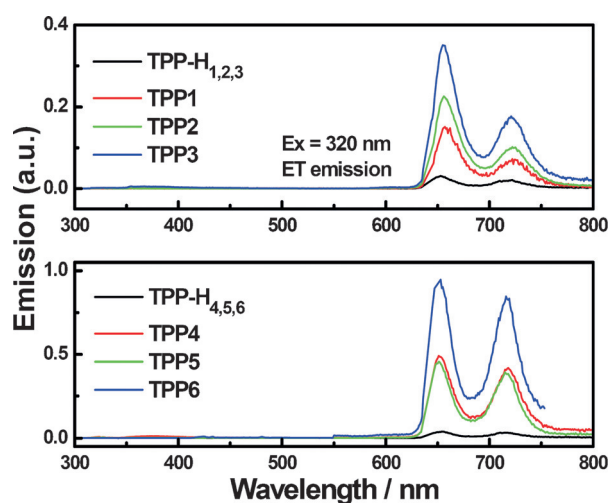
The energy transfer (ET) from fluorenyl donors toward the porphyrin acceptor was studied at room temperature in (aerated) dichloromethane in dilute solutions.

Figure 7 presents the emission spectra from 300 nm to 800 nm of **TPP1–TPP6** compared to those of the reference



**Figure 6.** Normalized absorption and emission spectra of *meta*-substituted porphyrins-based dendrimers **TPP4**, **TPP5**, **TPP6** and the corresponding reference compound **TPP-H<sub>4,5,6</sub>**.

compounds **TPP-H<sub>1,2,3</sub>** and **TPP-H<sub>4,5,6</sub>** upon excitation at 320 nm. Thus, by excitation of these molecules in their fluorene-based absorption, the emission spectra show only the typical emission of the porphyrin core (650 nm and 720 nm) and no residual dendron emission, meaning that the blue fluorenyl emission has been completely quenched for all these series. This suggests that the initial excitation energy of fluorenyl-containing antennae (320 nm) has been quantitatively transferred to the porphyrin core, resulting in the observed red emission at 650–720 nm. As expected, the reference compounds **TPP-H<sub>1,2,3</sub>** and **TPP-H<sub>4,5,6</sub>**, lacking this specific fluorene-based absorption, present almost no emission after 320 nm excitation.



**Figure 7.** Emission spectra for **TPP1–TPP6** upon excitation at the fluorene band.

### Luminescence quantum yields and lifetimes

The fluorescence quantum yields of these compounds were measured in dilute toluene solutions, taking **TPP** as standard. The quantum yields of **TPP1–TPP6** are listed in Table 2. The *para*-substituted series show around 20% quantum yield,

**Table 2.** Photophysical properties of the new dendrimers **TPP1–TPP6**.

Porphyrin	$\Phi_F$ [%] <sup>[b]</sup>	$\tau$ [ns] <sup>[c]</sup>	$k_{\text{obs}}$ [ $10^7 \text{ s}^{-1}$ ]	$k_f$ [ $10^7 \text{ s}^{-1}$ ] <sup>[a]</sup>	$\Sigma k_{\text{nr}}$ [ $10^7 \text{ s}^{-1}$ ] <sup>[a]</sup>
<b>TPP</b>	11	9.95	10.0	1.10	8.94
<b>TPP1</b>	20	9.79	10.2	2.04	8.17
<b>TPP2</b>	20	9.75	10.2	2.05	8.20
<b>TPP3</b>	19	9.72	10.3	1.95	8.33
<b>TPP4</b>	13	10.65	9.4	1.22	8.17
<b>TPP5</b>	11	10.77	9.3	1.02	8.26
<b>TPP6</b>	13	10.74	9.3	1.21	8.10

[a]  $k_f$  and  $\Sigma k_{\text{nr}}$  are the radiative rate constants and the sum of non-radiative decay constants, respectively, which were estimated from  $\Phi_F$  and  $\tau$  as described in the text. [b] Fluorescence quantum yields measured in distilled toluene using **TPP** ( $\Phi = 11\%$ ) as standard upon excitation at 426 nm. [c] Fluorescence lifetimes measured in dilute toluene, upon excitation at 426 nm.

higher than their parent molecule **TPP**, whereas *meta*-substituted porphyrins have quantum yields similar to that of the reference **TPP**.

In an attempt to determine the origin of the better emission efficiency for the *para* derivatives, the fluorescence lifetimes  $\tau$  were measured in dilute toluene solution.<sup>[20]</sup> Time-correlated single-photon counting using pulsed excitation at 426 nm was therefore employed and the resulting values are given in Table 2.

For the *para*-substituted series, slightly lower lifetimes (around 9.7 ns) were found than for *meta*-derivatives (around 10.7 ns). Also, whereas the former values are slightly lower than for **TPP**, the latter are higher. Assuming that the emissive state is formed with unitary efficiency in each case when each porphyrin derivative is excited directly into its Soret band at 426 nm, then:

$$\Phi_F = k_f/k_{\text{obs}}; \text{ in which } k_{\text{obs}} = (k_f + \sum k_{\text{nr}}) = \tau^{-1} \quad (1)$$

This equation [Eq. (1)] allows us to estimate the radiative rate constants  $k_f$  and the sum of the non-radiative decay constants  $\sum k_{\text{nr}}$  for each compound from the measured lifetime  $\tau$  and quantum yield  $\Phi_F$  (Table 2).<sup>[20]</sup> It is apparent that the introduction of the substituted dendrons on the *meso*-phenyl groups of the TPP core decrease the rate of non-radiative decay processes ( $\sum k_{\text{nr}}$ ) compared to **TPP**, regardless of their exact positions. In contrast, the radiative rate decay constants  $k_f$  appear more dependent on the substitution position,  $k_f$  decreasing by a factor of two upon going from first series **TPP1–TPP3** to the second one (**TPP4–TPP6**). Therefore, for the *para* series **TPP1–TPP3**, the enhanced quantum yields over **TPP** can be attributed almost exclusively to an increase of the oscillator strength of the emission, whereas the slightly improved quantum yields of the *meta*-substituted derivatives (**TPP4–TPP6**) are probably due to a less effective non-radiative decay.

### Two-photon absorption

As the fluorenyl-porphyrin dendrimers exhibit good fluorescence properties, their two-photon absorption cross-sections could be determined by investigating their two-photon excited fluorescence (TPEF) in dichloromethane, except for compounds bearing fluorenes devoid of alkyl chains, **TPP1** and **TPP4**, which were found to be not soluble enough in dichloromethane to perform TPEF measurements. Measurements were performed in  $10^{-4}$  M solutions, using a mode-locked titanium:sapphire laser delivering femtosecond pulses, following the experimental protocol described by Xu and Webb.<sup>[21]</sup>

A fully quadratic dependence of the fluorescence intensity on the excitation power was observed for each sample at all wavelengths of the spectra shown in Figure 8, indicating that the obtained cross-sections are only due to TPA. An example of this quadratic dependence is shown for compound **TPP2** at 790 nm in Figure 9.

An increase of the TPA cross-sections compared with that of **TPP** (12 GM at 790 nm) was observed for all the fluorenyl porphyrins (Table 3). These cross-sections were found to be more

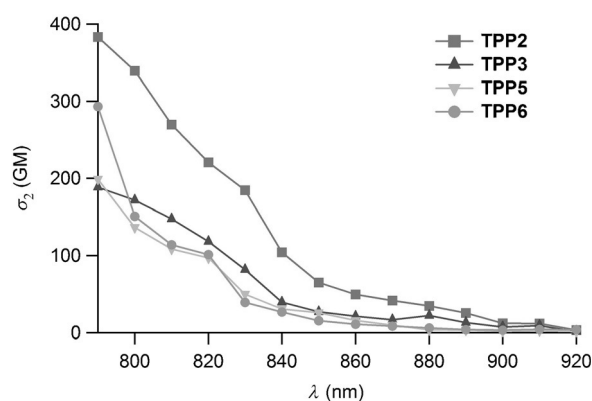


Figure 8. Two-photon absorption spectra of the dendrimers in dichloromethane.

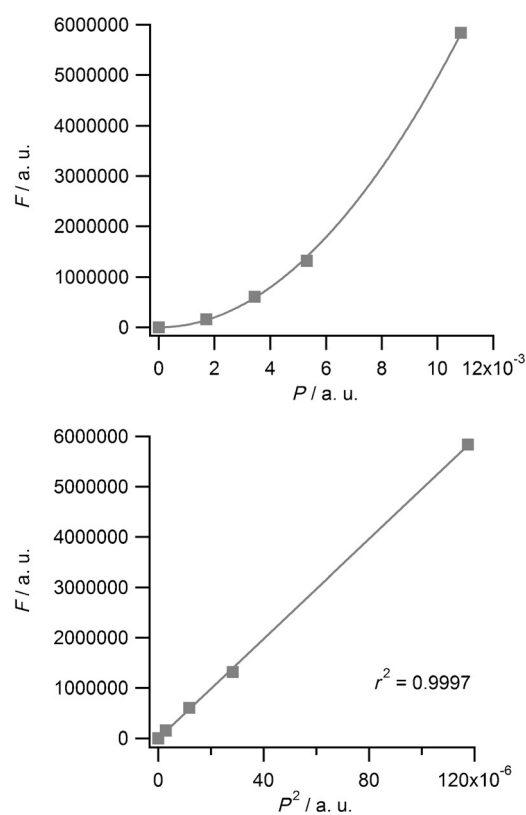


Figure 9. Top: quadratic dependence of the emission intensity ( $F$ ) on laser excitation power ( $P$ ) for compound **TPP2** at 790 nm. Bottom: dependence of  $F$  on  $P^2$ .

than one order of magnitude larger than that of **TPP**. Comparison between **TPP2** and **TPP5** reveals that one alkynylfluorenyl group at *para*-positions to each *meso*-phenylene groups of the porphyrin is much efficient for TPA than two such groups at *meta* positions, outlining the importance of cross-conjugation through the *meso*-phenylene groups, even if the  $\pi$ -conjugation between the dendrons and the porphyrin core is rather restricted.<sup>[22]</sup>

This increase of the TPA cross-sections combined to the increase of the fluorescence quantum yields leads to a very large

**Table 3.** Two-Photon absorption and brightness properties of the dendrimers.

Compound	Fluorenes/porphyrin	$\lambda_{\text{TPA}}^{\text{max}}$ [nm]	$\sigma_2^{\text{max}}$ [GM] <sup>[a]</sup>	$\Phi_{\text{f}}\sigma_2^{\text{max}}$ [GM] <sup>[b]</sup>	Two-photon brightness enhancement factor <sup>[c]</sup>
TPP	0	790	12 <sup>[d]</sup>	1.3	1
TPP1 <sup>[e]</sup>	4	–	–	–	–
TPP2	4	790	380	76	59
TPP3	8	790	190	36	28
TPP4 <sup>[e]</sup>	8	–	–	–	–
TPP5	8	790	200	20	15
TPP6	16	790	290	38	29

[a] Intrinsic TPA cross-sections measured in  $10^{-4}$  M dichloromethane solutions by TPEF in the femtosecond regime; a fully quadratic dependence of the fluorescence intensity on the excitation power is observed and TPA responses are fully non-resonant. [b] Maximum two-photon brightness in dichloromethane. [c]  $\Phi_{\text{f}}\sigma_2^{\text{max}}$  factor relative to that of TPP. [d] Data from reference [25]. [e] Compounds bearing unsubstituted fluorenes (TPP1 and TPP4) were not soluble enough in dichloromethane to perform TPEF measurements.

enhancement of the two-photon brightness  $\sigma_2\Phi_{\text{f}}$  of dendrimers over that of TPP. This figure of merit is thus enhanced by a factor ranging between 15 for TPP5 and 59 for TPP2 (Table 3), which is quite appealing for imaging purposes in the perspective of theranostic applications (i.e., combining two-photon fluorescence imaging and photodynamic therapy). It should be emphasized that even higher TPA cross-sections have already been obtained with other porphyrin systems,<sup>[23]</sup> exhibiting more efficient conjugation between the subchromophoric moieties, but generally along with strong modifications of the other photophysical properties, which limit their interest for theranostic applications. Indeed, such compounds usually exhibit a modest to negligible fluorescence, as well as interfering residual one-photon absorption (OPA), which leads to the loss of some advantages of selective TPA, mainly the 3D resolution. In contrast, fluorenyl-porphyrin dendrimers exhibit an improved trade-off<sup>[24]</sup> between selective (non-resonant) TPA cross-sections and fluorescence properties.

### Oxygen sensitization

The quantum yields of singlet oxygen generation were determined for fluorenyl-porphyrin dendrimers TPP1–TPP6 (Table 4). Interestingly, they are higher or comparable to that of TPP, revealing that for these compounds, the increase of the fluorescence efficiency is not obtained at the expense of the singlet oxygen production. This also confirms that the increase of the fluorescence quantum yield observed for the *para* series is mostly due to an increase of the radiative rate constant, rather than a decrease of the intersystem crossing rate constant (the singlet oxygen quantum yield of which is related).

Combined with the increase of the TPA cross-sections, such behavior leads to strong enhancements of the figure of merit of the two-photon excited oxygen sensitization ( $\Phi_{\Delta}\sigma_2^{\text{max}}$ ) in comparison with that of TPP. A remarkable 37-fold enhancement factor was obtained for *para*-substituted TPP2, whereas 16- to 23-fold enhancements were obtained for the other den-

**Table 4.** Oxygen sensitization properties of the new dendrimers TPP1–TPP6.

Compound	$\Phi_{\Delta}$ <sup>[a]</sup>	$\Phi_{\Delta}\sigma_2^{\text{max}}$ [GM] <sup>[b]</sup>	Two-photon excited oxygen sensitization enhancement factor <sup>[c]</sup>
TPP	0.60	7.2	1
TPP1	0.69	–	–
TPP2	0.70	266	37
TPP3	0.65	124	17
TPP4	0.61	–	–
TPP5	0.59	118	16
TPP6	0.56	162	23

[a] Singlet oxygen production quantum yield determined relative to TPP in dichloromethane ( $\Phi_{\Delta}[\text{TPP}] = 0.60$ ). [b]  $\Phi_{\Delta}\sigma_2^{\text{max}}$ : figure of merit of the two-photon excited singlet oxygen production in dichloromethane. [c] Enhancement factor:  $\Phi_{\Delta}\sigma_2^{\text{max}}$  of the compound normalized to that of TPP.

drimers (Table 4). These compounds are therefore well suited for two-photon sensitizing applications, and taking into account their fluorescence properties, for theranostic applications combining two-photon fluorescence imaging and photodynamic therapy, provided that hydrophilicity and biocompatibility of the systems are improved, which might be achieved for example, by introducing oligoethyleneglycol chains on the fluorenes.

### Conclusions

Six new conjugated dendrimers TPP1–TPP6 with terminal fluorenyl units in phenyl-alkynyl-containing dendrons were synthesized and characterized. Variations of the position (*para* or *meta*) of the dendron branching on the *meso*-phenyl rings of the TPP core significantly influence the spectroscopic properties of the final porphyrin dendrimers, as well as the number of terminal 2-fluorene groups in each dendron. For all derivatives, the absence of blue emission from the fluorene chromophore upon excitation in the band near 330 nm indicates that the energy transfer from the peripheral fluorene-containing antennae to the central porphyrin core is nearly quantitative, regardless of the number of fluorene groups in the peripheral dendrons and of their branching point at the *meso*-phenyl rings. However, for the *para*-functionalized series TPP1–TPP3, larger luminescence quantum yields are observed than for the *meta*-substituted ones, especially when comparison is made between compounds containing a similar number of terminal 2-fluorene groups in each branch. Due to the presence of two branching positions in the *meta*-series, a comparably larger number of 2-fluorene groups are present in TPP4–TPP6 relative to TPP1–TPP3, respectively. As a result, the brightest compound of this series is TPP6, whereas TPP3, albeit less bright, combines the highest luminescence quantum yield with a remarkable light-harvesting power. Further studies on energy transfer process are ongoing on related analogues to optimize further the light-harvesting properties.

In comparison with reference TPP, both *para* and *meta*-substituted compounds exhibit intrinsic two-photon absorption cross-sections enhanced by at least one order of magnitude,

together with higher or maintained singlet oxygen quantum yields. *Para*-substituted dendrimer **TPP2** combines the largest enhancements of both two-photon brightness and two-photon singlet oxygen production. Such kind of molecular engineering is therefore also very promising for theranostic applications combining two-photon fluorescence imaging and photodynamic therapy.

## Experimental section

### General

Unless otherwise stated, all solvents used in reactions were distilled using common purification protocols,<sup>[26]</sup> except DMF and *i*Pr<sub>2</sub>NH, which were dried on molecular sieves (3 Å). Compounds were purified by chromatography on silica gel using different mixtures of eluents as specified. <sup>1</sup>H and <sup>13</sup>C NMR spectra were recorded on BRUKER Ascend 400 and 500 at 298 K. The chemical shifts are referenced to internal tetramethylsilane. High-resolution mass spectra were recorded on a Bruker MicroTOF-Q II (for compounds **TPP 1**, **TPP2**, and **TPP4**) and a Thermo Fisher Scientific Q-Exactive (for compounds **TPP 3** and **TPP 6**) in ESI positive mode at CRMPO in Rennes. Reagents were purchased from commercial suppliers and used as received. 3,5-bis(trimethylsilyl)ethynylbenzaldehyde,<sup>[27]</sup> 2-ethynylfluorene (**1**),<sup>[28]</sup> 2-ethynyl-9,9-dibutyl-fluorene (**2**),<sup>[29]</sup> 4-((9,9-dibutyl-fluoren-2-yl) ethynyl)benzaldehyde (**4**),<sup>[15]</sup> 3,5-bis((9,9-dibutyl-fluoren-2-yl) ethynyl) benzaldehyde (**6**),<sup>[15]</sup> 2,2'-(5-ethynyl-1,3-phenylene) bis(ethyne-2,1-diyl) bis(9,9-dibutyl-fluoren-2-yl) (**7**),<sup>[15]</sup> and **TPP-H**<sub>1,2,3</sub><sup>[18a]</sup> were obtained following published preparations.

### Organic precursor synthesis

**4-((Fluoren-2-yl)ethynyl)benzaldehyde (3)**: In a Schlenk tube, a mixture of commercial 2-(4-bromophenyl)-1,3-dioxolane (1.04 g, 4.54 mmol, 1 equiv), **1** (1.0 g, 5.26 mmol, 1.15 equiv), [Pd(PPh<sub>3</sub>)<sub>2</sub>Cl<sub>2</sub>] (18.4 mg, 0.026 mmol, 0.6% equiv) and CuI (2.5 mg, 0.013 mmol, 0.3% equiv) were stirred in DMF (6 mL) and *i*Pr<sub>2</sub>NH (6 mL) was added under argon. The reaction medium was degassed by freeze–pump–thaw twice and heated for two days at 95 °C. After evaporation of the volatiles, residue was purified by chromatography using a heptane/CH<sub>2</sub>Cl<sub>2</sub> (5:1) mixture. The intermediate 2-(4-((fluoren-2-yl)ethynyl)-phenyl)-1,3-dioxolane, a yellow powder, was not isolated. This crude sample was added into THF (20 mL) and aqueous HCl (5 mL, 10% aq.), then this mixture was stirred 12 h at 25 °C. The reaction was neutralized by NaHCO<sub>3</sub> and extracted with CH<sub>2</sub>Cl<sub>2</sub> and water. After evaporation of the volatiles, the residue was purified by chromatography using a heptane/CH<sub>2</sub>Cl<sub>2</sub> (4:1) mixture as eluent. The title compound **3** was isolated as a yellow powder (613 mg, 48% overall yield). <sup>1</sup>H NMR (400 MHz, CDCl<sub>3</sub>): δ = 10.03 (s, 1H), 7.88 (d, *J* = 8.4 Hz, 2H), 7.80 (t, *J* = 7.4 Hz, 2H), 7.74 (s, 1H), 7.69 (d, *J* = 8.4 Hz, 2H), 7.58 (t, *J* = 7.6 Hz, 2H), 7.41 (t, *J* = 7.2 Hz, 1H), 7.34 (t, *J* = 7.4 Hz, 1H), 3.94 ppm (s, 2H); HRMS: *m/z* calcd for C<sub>22</sub>H<sub>14</sub>NaO: 317.0942 [*M* + Na]<sup>+</sup>; found: 317.0942.

**3,5-Bis((fluoren-2-yl)ethynyl)benzaldehyde (5)**: In a Schlenk tube, a mixture of commercial 2-(3,5-dibromophenyl)-1,3-dioxolane (1.02 g, 3.31 mmol, 1 equiv), **1** (1.58 g, 8.28 mmol, 2.5 equiv), [Pd(PPh<sub>3</sub>)<sub>2</sub>Cl<sub>2</sub>] (28 mg, 0.04 mmol, 1.2% equiv), and CuI (4 mg, 0.02 mmol, 0.6% equiv) was stirred in DMF (5 mL) and *i*Pr<sub>2</sub>NH (5 mL) was added under argon. The reaction medium was degassed by freeze–pump–thaw twice and heated for two days at 95 °C. After evaporation of the volatiles, the residue was purified by chromatography using a heptane/CH<sub>2</sub>Cl<sub>2</sub> (5:1) mixture as

eluent. The intermediate compound 2-(3,5-bis((fluoren-2-yl) ethynyl)phenyl)-1,3-dioxolane) was not isolated from the yellow powder. This crude product was dissolved into a mixture of THF (40 mL) and aqueous HCl (10 mL, 10% aq.), then this mixture was stirred 10 h at 25 °C. The reaction was neutralized by NaHCO<sub>3</sub> and extracted with CH<sub>2</sub>Cl<sub>2</sub> and water. After evaporation of the volatiles, the residue was purified by chromatography using a mixture of heptane/CH<sub>2</sub>Cl<sub>2</sub> (1:1) as eluent. The title compound **5** was isolated as a yellow powder (900 mg, 56% overall yield). <sup>1</sup>H NMR (400 MHz, CDCl<sub>3</sub>): δ = 10.04 (s, 1H), 7.99 (d, *J* = 1.6 Hz, 2H), 7.96 (t, *J* = 1.2 Hz, 1H), 7.81 (t, *J* = 6.8 Hz, 4H), 7.74 (s, 2H), 7.58 (t, *J* = 6.4 Hz, 4H), 7.41 (t, *J* = 7.4 Hz, 2H), 7.35 (t, *J* = 7.4 Hz, 2H), 3.95 ppm (s, 4H). HRMS: *m/z* calcd for C<sub>37</sub>H<sub>23</sub>O: 482.1665 [*M* + H]<sup>+</sup>; found: 482.1669

**4-((3,5-Bis((9,9-dibutyl-9H-fluoren-2-yl)ethynyl)phenyl)ethynyl)benzaldehyde (8)**: In a Schlenk tube, a mixture of 4-bromobenzaldehyde (123 mg, 0.67 mmol, 1 equiv), **7** (515 mg, 0.73 mmol, 1.1 equiv), [Pd(PPh<sub>3</sub>)<sub>2</sub>Cl<sub>2</sub>] (28 mg, 0.04 mmol, 6% equiv), and CuI (4 mg, 0.02 mmol, 3% equiv) were added DMF (5 mL) and *i*Pr<sub>2</sub>NH (10 mL) under argon. Then the system was degassed by freeze–pump–thaw twice and heated for two days at 95 °C. After being evaporated, residue was absorbed in silica and further purified by chromatography (heptane/CH<sub>2</sub>Cl<sub>2</sub> = 5:1), showing white powder (357 mg, 66% yield). <sup>1</sup>H NMR (400 MHz, CDCl<sub>3</sub>): δ = 10.05 (s, 1H), 7.90 (d, *J* = 8.4 Hz, 2H), 7.78 (s, 1H), 7.72–7.69 (m, 8H), 7.54–7.52 (m, 4H), 7.38–7.33 (m, 6H), 1.99 (t, *J* = 8.0 Hz, 8H), 1.14–1.05 (m, 8H), 0.69 (t, *J* = 7.2 Hz, 12H), 0.64–0.53 ppm (m, 8H); HRMS: *m/z* calcd for C<sub>61</sub>H<sub>58</sub>O: 806.4482 [*M*]<sup>+</sup>; found: 806.4481.

**3,5-Bis((3,5-bis((9,9-dibutyl-fluoren-2-yl)ethynyl)phenyl)ethynyl)benzaldehyde (9)**: In a Schlenk tube, a mixture of 3,5-dibromobenzaldehyde (160 mg, 0.61 mmol, 1 equiv), **7** (900 mg, 1.28 mmol, 2.1 equiv), [Pd(PPh<sub>3</sub>)<sub>2</sub>Cl<sub>2</sub>] (51 mg, 0.07 mmol, 6% equiv) and CuI (7 mg, 0.04 mmol, 3% equiv) were stirred in DMF (15 mL) and *i*Pr<sub>2</sub>NH (20 mL) was added under argon. The system was degassed by freeze–pump–thaw twice and heated for two days at 95 °C. After evaporation of the volatiles, the residue was absorbed on silica and purified by chromatography using a heptane/CH<sub>2</sub>Cl<sub>2</sub> (5:1) mixture as eluent. The title product was isolated as a white powder (530 g, 58% yield). <sup>1</sup>H NMR (400 MHz, CDCl<sub>3</sub>): δ = 10.06 (s, 1H), 8.02 (s, 2H), 7.95 (s, 1H), 7.79 (s, 2H), 7.73–7.70 (m, 11H), 7.55–7.53 (m, 9H), 7.38–7.31 (m, 12H), 2.00 (t, *J* = 8 Hz, 16H), 1.06–0.98 (m, 16H), 0.64–0.46 ppm (m, 40H); HRMS: *m/z* calcd for C<sub>115</sub>H<sub>110</sub>O: 1506.8600 [*M*]<sup>+</sup>; found: 1506.6780.

### Porphyrin synthesis

Reference porphyrin **TPP-H**<sub>1,2,3</sub> for **TPP1**, **TPP2** and **TPP3**, was synthesized as described earlier by our group.<sup>[18a]</sup>

**TPP-H**<sub>4,5,6</sub>: A mixture of 3,5-bis(trimethylsilyl)ethynylbenzaldehyde (1 g, 3.35 mmol, 1 equiv) and propionic acid (15 mL) was heated at 120 °C. After reaching that temperature, pyrrole (0.23 mL, 3.35 mmol, 1 equiv) in propionic acid (1 mL) was added dropwise into the mixture and the reaction medium was heated at reflux for 3.3 h. After cooling to room temperature, MeOH was added to the reaction mixture and the precipitate was filtered. The residue could be purified by chromatography (heptane/CH<sub>2</sub>Cl<sub>2</sub> = 5:1), giving intermediate **TPP-TMS**<sub>4,5,6</sub> as a red powder (260 mg, 22% yield). <sup>1</sup>H NMR (400 MHz, CDCl<sub>3</sub>): δ = 8.86 (s, 8H), 8.27 (s, 8H), 8.07 (s, 4H), 0.30 (s, 72H), –2.91 ppm (s, 2H). Then intermediate **TPP-TMS**<sub>4,5,6</sub> (550 mg, 0.40 mmol, 1 equiv) was added into a mixture solvents of CH<sub>2</sub>Cl<sub>2</sub> (90 mL) and MeOH (30 mL), together with K<sub>2</sub>CO<sub>3</sub> (877 mg, 6.36 mmol, 16 equiv). This mixture was stirred for 1 day at room temperature. After being evaporated, residue was further purified by chromatography (heptane/CH<sub>2</sub>Cl<sub>2</sub> = 2:1), giving the de-

sired **TPP-H<sub>4,5,6</sub>** as a purple powder (274 mg, 86% yield). <sup>1</sup>H NMR (400 MHz, CDCl<sub>3</sub>): δ = 8.85 (s, 8H), 8.31 (s, 8H), 8.06 (s, 4H), 3.20 (s, 8H), -2.92 ppm (s, 2H); HRMS: *m/z* calcd for C<sub>60</sub>H<sub>31</sub>N<sub>4</sub>: 807.25487 [M+H]<sup>+</sup>; found: 807.25410.

**TPP1:** A mixture of **3** (400 mg, 1.36 mmol, 1 equiv) and propionic acid (5 mL) was heated at 120 °C. After reaching that temperature, pyrrole (0.095 mL, 1.36 mmol, 1 equiv) in propionic acid (1 mL) was added dropwise into the mixture and the reaction was heated at reflux for 1.5 h. After cooling down at room temperature, MeOH was added and the reaction medium was filtered. The solid residue was then purified by chromatography using a petroleum ether/CH<sub>2</sub>Cl<sub>2</sub> (5:1) mixture as eluent. The title compound was isolated as a purple powder (80 mg, 17% yield). <sup>1</sup>H NMR (400 MHz, CDCl<sub>3</sub>, ppm): δ = 8.92 (s, 8H), 8.24 (d, *J* = 7.2 Hz, 8H), 7.97 (d, *J* = 7.2 Hz, 8H), 7.88–7.85 (m, 12H), 7.73 (d, *J* = 8 Hz, 4H), 7.60 (d, *J* = 6.4 Hz, 4H), 7.43 (t, *J* = 6.8 Hz, 4H), 7.36 (t, *J* = 6.8 Hz, 4H), 4.00 (s, 8H), -2.74 ppm (s, 2H); UV/Vis (CH<sub>2</sub>Cl<sub>2</sub>): λ<sub>max</sub> = 320, 426, 518, 554, 592, 650 nm; HRMS: *m/z* calcd for C<sub>104</sub>H<sub>63</sub>N<sub>4</sub>: 1366.4974 [M+H]<sup>+</sup>; found: 1367.5200; elemental analysis calcd (%) for C<sub>104</sub>H<sub>62</sub>N<sub>4</sub>: C 91.33, H 4.57, N 4.10; found: C 91.06, H 4.39, N 4.08.

**TPP2:** A mixture of aldehyde **4** (700 mg, 1.72 mmol, 1 equiv) and propionic acid (6.5 mL) was heated to 120 °C. After dropwise addition of a solution of pyrrole (0.12 mL, 1.72 mmol, 1 equiv) in propionic acid (1.0 mL), the reaction medium was heated at reflux for a further 1.5 h. After cooling at room temperature, MeOH was added to the reaction mixture and the precipitate was filtered. The residue could be purified by repeated chromatography on silica using petroleum ether/CH<sub>2</sub>Cl<sub>2</sub> (1:1) as eluent. The title compound was isolated as a rose-purple powder (220 mg, 28% yield). <sup>1</sup>H NMR (400 MHz, CDCl<sub>3</sub>): δ = 8.92 (s, 8H), 8.24 (d, <sup>3</sup>*J*<sub>HH</sub> = 7.6 Hz, 8H), 7.99 (d, <sup>3</sup>*J*<sub>HH</sub> = 7.6 Hz, 8H), 7.78–7.75 (m, 8H), 7.69–7.67 (m, 8H), 7.40–7.35 (m, 12H), 2.05 (t, <sup>3</sup>*J*<sub>HH</sub> = 8.0 Hz, 16H), 1.19–1.10 (m, 16H), 0.73 (t, <sup>3</sup>*J*<sub>HH</sub> = 7.2 Hz, 24H), 0.69–0.60 (m, 16H), -2.74 ppm (s, 2H); <sup>13</sup>C{<sup>1</sup>H} NMR (100 MHz, CDCl<sub>3</sub>): δ = 151.1 (s), 150.9 (s), 141.9 (s), 141.7 (s), 140.4 (s), 134.6 (s), 130.8 (s), 130.0 (s), 127.6 (s), 126.9 (s), 126.1 (s), 123.1 (s), 122.9 (s), 121.4 (s), 120.1 (s), 119.7 (s), 91.9 (s), 89.3 (s), 55.1 (s), 40.2 (s), 26.0 (s), 23.1 (s), 13.9 ppm (s); UV/Vis (CH<sub>2</sub>Cl<sub>2</sub>): λ<sub>max</sub> (ε) = 323 (178.4), 427 (670.2), 519 (36.0), 556 (30.1), 592 (17.2), 649 nm (17.1 × 10<sup>3</sup> m<sup>-1</sup> cm<sup>-1</sup>); HRMS: *m/z* calcd for C<sub>136</sub>H<sub>127</sub>N<sub>4</sub>: 1815.9982 [M+H]<sup>+</sup>; found: 1816.0055; elemental analysis calcd (%) for C<sub>136</sub>H<sub>126</sub>N<sub>4</sub>: C 89.92, H 6.99, N 3.08; found: C 89.65, H 6.59, N 3.12.

**TPP3:** A mixture of aldehyde **8** (312 mg, 0.39 mmol, 1 equiv) and propionic acid (2 mL) was heated to 120 °C. After dropwise addition of a solution of pyrrole (0.03 mL, 0.39 mmol, 1 equiv) in propionic acid (0.5 mL), the reaction medium was heated at reflux for a further 5.5 h. After cooling to room temperature, MeOH was added to the reaction mixture and the precipitate was filtered. The residue could be purified by repeated chromatography on silica using petroleum ether/CH<sub>2</sub>Cl<sub>2</sub> (5:1) as eluent. The title compound was initially isolated as red powder, and subsequently recrystallized from hot CHCl<sub>3</sub> solutions upon addition of excess MeOH, giving eventually the title compound as a dark-purple powder (72 mg, 22% yield). <sup>1</sup>H NMR (400 MHz, CDCl<sub>3</sub>, ppm): δ = 8.94 (s, 8H), 8.28 (d, <sup>3</sup>*J*<sub>HH</sub> = 8.0 Hz, 8H), 7.99 (d, <sup>3</sup>*J*<sub>HH</sub> = 8.0 Hz, 8H), 7.87 (s, 8H), 7.83 (s, 4H), 7.73 (d, <sup>3</sup>*J*<sub>HH</sub> = 8.0 Hz, 16H), 7.59–7.57 (m, 16H), 7.39–7.32 (m, 24H), 2.02 (t, <sup>3</sup>*J*<sub>HH</sub> = 8.0 Hz, 32H), 1.17–1.08 (m, 32H), 0.71 (t, <sup>3</sup>*J*<sub>HH</sub> = 7.2 Hz, 48H), 0.67–0.58 (m, 32H), -2.72 ppm (s, 2H); <sup>13</sup>C{<sup>1</sup>H} NMR (100 MHz, CDCl<sub>3</sub>): δ = 151.1 (s), 150.8 (s), 142.4 (s), 141.8 (s), 140.3 (s), 134.7 (s), 134.2 (s), 134.0 (s), 130.7 (s), 130.2 (s), 127.6 (s), 126.9 (s), 126.1 (s), 124.4 (s), 124.1 (s), 124.0 (s), 122.9 (s), 122.6 (s), 120.9 (s), 120.1 (s), 119.7 (s), 91.9 (s), 90.4 (s), 89.3 (s), 87.9 (s), 55.1 (s), 40.2 (s), 25.9 (s), 23.1 (s), 13.8 ppm (s); UV/Vis (CH<sub>2</sub>Cl<sub>2</sub>): λ<sub>max</sub> (ε) = 329

(486.6), 347 (484.9), 425 (707.1), 519 (34.5), 555 (27.4), 593 (15.8), 649 nm (15.4 × 10<sup>3</sup> m<sup>-1</sup> cm<sup>-1</sup>); HRMS: *m/z* calcd for C<sub>260</sub>H<sub>239</sub>N<sub>4</sub>: 3416.8819 [M+H]<sup>+</sup>; found: 3416.8821; elemental analysis calcd (%) for C<sub>260</sub>H<sub>238</sub>N<sub>4</sub>: C 91.34, H 7.02, N 1.64; found: C 91.05, H 6.93, N 1.77.

**TPP4:** A mixture of **5** (850 mg, 1.76 mmol, 1 equiv) and propionic acid (40 mL) was heated at 120 °C. After reaching that temperature, pyrrole (0.12 mL, 1.76 mmol, 1 equiv) in propionic acid (1 mL) was added dropwise into the mixture and the reaction was heated at reflux for 3 h. After cooling down at room temperature, MeOH was added and the reaction medium was filtered and washed further with MeOH. The solid residue was recrystallized by CH<sub>2</sub>Cl<sub>2</sub>. The title compound was isolated as a light-brown powder (20 mg, 2% yield). <sup>1</sup>H NMR (400 MHz, CDCl<sub>3</sub>): 9.03 (s, 8H), 8.42 (s, 8H), 8.20 (s, 4H), 7.78–7.76 (m, 24H), 7.62 (d, *J* = 8.8 Hz, 8H), 7.53 (d, *J* = 7.6 Hz, 8H), 7.38 (t, *J* = 7.6 Hz, 8H), 7.31 (t, *J* = 7.2 Hz, 8H), 3.91 (s, 16H), -2.75 ppm (s, 2H); UV/Vis (CH<sub>2</sub>Cl<sub>2</sub>): λ<sub>max</sub> = 324, 428, 517, 552, 589, 646 nm; HRMS: *m/z* calcd for C<sub>164</sub>H<sub>95</sub>N<sub>4</sub>: 2118.7478 [M+H]<sup>+</sup>; found: 2119.7510; elemental analysis calcd (%) for C<sub>164</sub>H<sub>94</sub>N<sub>4</sub>: C 92.89, H 4.47, N 2.64; found: C 92.48, H 4.44, N 2.59.

**TPP5:** A mixture of aldehyde **6** (860 mg, 1.22 mmol, 1 equiv) and propionic acid (6 mL) was heated to 120 °C. After dropwise addition of a solution of pyrrole (0.085 mL, 1.22 mmol, 1 equiv) in propionic acid (1.0 mL), the reaction medium was heated at reflux for a further 3.0 h. After cooling to room temperature, MeOH was added to the reaction mixture and the precipitate was filtered. The residue could be purified by repeated chromatography on silica using petroleum ether/CH<sub>2</sub>Cl<sub>2</sub> (5:1) as eluent. The title compound was isolated as red powder, and subsequently recrystallized from hot CHCl<sub>3</sub> solutions upon addition of excess MeOH (165 mg, 18% yield). <sup>1</sup>H NMR (400 MHz, CDCl<sub>3</sub>): δ = 9.02 (s, 8H), 8.43 (s, 8H), 8.26 (s, 4H), 7.67 (d, <sup>3</sup>*J*<sub>HH</sub> = 7.2 Hz, 16H), 7.59–7.57 (m, 16H), 7.31 (broad, 24H), 1.95 (t, <sup>3</sup>*J*<sub>HH</sub> = 8.0 Hz, 32H), 1.07–1.02 (m, 32H), 0.65–0.48 (m, 80H), -2.75 ppm (s, 2H); <sup>13</sup>C{<sup>1</sup>H} NMR (100 MHz, CDCl<sub>3</sub>): δ = 151.1 (s), 150.8 (s), 142.5 (s), 141.8 (s), 140.3 (s), 136.7 (s), 134.0 (s), 130.8 (s), 127.6 (s), 126.9 (s), 126.2 (s), 122.9 (s), 122.6 (s), 121.0 (s), 120.0 (s), 119.7 (s), 118.7 (s), 91.6 (s), 88.6 (s), 55.1 (s), 40.1 (s), 25.9 (s), 23.0 (s), 13.8 ppm (s); UV/Vis (CH<sub>2</sub>Cl<sub>2</sub>): λ<sub>max</sub> (ε) = 327 (393.5), 427 (806.6), 517 (50.8), 551 (30.9), 590 (27.8), 646 nm (22.4 × 10<sup>3</sup> m<sup>-1</sup> cm<sup>-1</sup>); HRMS: *m/z* calcd for C<sub>228</sub>H<sub>223</sub>N<sub>4</sub>: 3016.7567 [M+H]<sup>+</sup>; found: 3016.7647; elemental analysis calcd (%) for C<sub>228</sub>H<sub>222</sub>N<sub>4</sub>: C 90.73, H 7.41, N 1.86; found: C 90.39, H 7.38, N 1.93.

**TPP6:** A mixture of aldehyde **9** (500 mg, 0.33 mmol, 1 equiv) and propionic acid (3 mL) was heated to 120 °C. After dropwise addition of a solution of pyrrole (0.085 mL, 1.22 mmol, 1 equiv) in propionic acid (0.5 mL), the reaction medium was heated at reflux for a further 5.5 h. After cooling to room temperature, MeOH was added to the reaction mixture and the precipitate was filtered. The residue could be purified by repeated chromatography on silica using petroleum ether/CH<sub>2</sub>Cl<sub>2</sub> (5:1) as eluent. The title compound was initially isolated as red powder, and subsequently recrystallized from hot CHCl<sub>3</sub> solutions upon addition of excess MeOH, giving eventually the desired compound **1d** as a dark-purple powder (66 mg, 13% yield). <sup>1</sup>H NMR (400 MHz, CDCl<sub>3</sub>): δ = 9.08 (s, 8H), 8.46 (s, 8H), 8.22 (s, 4H), 7.77–7.74 (m, 20H), 7.65–7.61 (m, 32H), 7.52–7.47 (m, 36H), 7.36–7.28 (m, 48H), 1.91 (t, <sup>3</sup>*J*<sub>HH</sub> = 8.0 Hz, 64H), 1.05–0.99 (m, 64H), 0.63–0.52 (m, 160H), -2.70 ppm (s, 2H); <sup>13</sup>C{<sup>1</sup>H} NMR (100 MHz, CDCl<sub>3</sub>): δ = 151.0 (s), 150.8 (s), 141.8 (s), 140.3 (s), 134.4 (s), 134.0 (s), 130.7 (s), 127.6 (s), 126.8 (s), 126.1 (s), 124.4 (s), 124.0 (s), 123.6 (s), 122.9 (s), 122.2 (s), 120.8 (s), 120.0 (s), 119.6 (s), 91.9 (s), 89.4 (s), 89.1 (s), 87.8 (s), 55.0 (s), 40.1 (s), 25.8 (s), 23.0 (s), 13.8 ppm (s); UV/Vis (CH<sub>2</sub>Cl<sub>2</sub>): λ<sub>max</sub> (ε) = 327 (916.6), 348 (821.6), 426 (566.1), 517 (27.8), 551 (14.9), 590 (12.9), 645 nm (9.3 ×

$10^3 \text{ M}^{-1} \text{ cm}^{-1}$ ); HRMS:  $m/z$  calcd for  $\text{C}_{476}\text{H}_{448}\text{N}_4$ : 3109.7584 [ $M+2\text{H}$ ] $^{2+}$ ; found: 3109.7570; elemental analysis calcd (%) for  $\text{C}_{476}\text{H}_{448}\text{N}_4$ : C 91.88, H 7.22, N 0.90; found: C 91.67, H 7.17, N 0.72.

### Spectroscopic measurements

All photophysical properties have been performed with freshly-prepared air-equilibrated solutions at room temperature (298 K). UV/Vis absorption spectra were recorded on a BIO-TEK instrument UVIKON XL spectrometer or on a Jasco V-570 spectrophotometer. Fluorescence measurements were performed using an Edinburgh Instruments (FLS920) spectrometer in photon-counting mode. Steady-state and time-resolved fluorescence measurements were performed on dilute solutions (ca.  $10^{-6} \text{ M}$ , optical density  $< 0.1$ ) contained in standard 1 cm quartz cuvettes using an Edinburgh Instruments (FLS920) spectrometer in photon-counting mode. Fully corrected emission spectra were obtained, for each compound, under excitation at the wavelength of the absorption maximum, with  $A_{\lambda, \text{ex}} < 0.1$  to minimize internal absorption. Fluorescence lifetimes were measured by time-correlated single photon counting (TCSPC). Excitation was achieved by a hydrogen-filled nanosecond flashlamp (repetition rate 40 kHz). The instrument response (FWHM ca. 1 ns) was determined by measuring the light scattered by a Ludox suspension. The TCSPC traces were analyzed by standard iterative deconvolution methods implemented in the software of the fluorimeter. All compounds displayed monoexponential fluorescence decays. The reported lifetimes are within  $\pm 0.1 \text{ ns}$ .

### Measurements of singlet oxygen quantum yield ( $\Phi_{\Delta}$ )

Measurements were performed on a Fluorolog-3 (Horiba-Jobin-Yvon), using a 450 W Xenon lamp. The emission at 1272 nm was detected using a liquid nitrogen-cooled Ge-detector model (EO-817 L, North Coast Scientific Co). Singlet oxygen quantum yields  $\Phi_{\Delta}$  were determined in dichloromethane solutions, using tetraphenylporphyrin (TPP) in dichloromethane as reference solution ( $\Phi_{\Delta}[\text{TPP}] = 0.60$ ) and were estimated from  $^1\text{O}_2$  luminescence at 1272 nm.

### Two-photon absorption experiments

To span the 790–920 nm range, a Nd:YLF-pumped Ti:sapphire oscillator (Chameleon Ultra, Coherent) was used generating 140 fs pulses at a 80 MHz rate. The excitation power is controlled using neutral density filters of varying optical density mounted in a computer-controlled filter wheel. After fivefold expansion through two achromatic doublets, the laser beam is focused by a microscope objective (10 $\times$ , NA 0.25, Olympus, Japan) into a standard 1 cm absorption cuvette containing the sample. The applied average laser power arriving at the sample is typically between 0.5 and 40 mW, leading to a time-averaged light flux in the focal volume on the order of 0.1–10  $\text{mW m}^{-2}$ . The fluorescence from the sample is collected in epifluorescence mode, through the microscope objective, and reflected by a dichroic mirror (Chroma Technology Corporation, USA; “blue” filter set: 675dxcru; “red” filter set: 780dxcrr). This makes it possible to avoid the inner filter effects related to the high dye concentrations used ( $10^{-4} \text{ M}$ ) by focusing the laser near the cuvette window. Residual excitation light is removed using a barrier filter (Chroma Technology; “blue”: e650–2p, “red”: e750 sp–2p). The fluorescence is coupled into a 600  $\mu\text{m}$  multimode fiber by an achromatic doublet. The fiber is connected to a compact CCD-based spectrometer (BTC112-E, B&WTEK, USA), which measures the two-photon excited emission spectrum. The emission spectra are corrected for the wavelength-dependence of the detec-

tion efficiency using correction factors established through the measurement of reference compounds having known fluorescence emission spectra. Briefly, the set-up allows for the recording of corrected fluorescence emission spectra under multiphoton excitation at variable excitation power and wavelength. TPA cross sections ( $\sigma_2$ ) were determined from the two-photon excited fluorescence (TPEF) cross sections ( $\sigma_2\Phi_{\text{F}}$ ) and the fluorescence emission quantum yield ( $\Phi_{\text{F}}$ ). TPEF cross sections of  $10^{-4} \text{ M}$  dichloromethane solutions were measured relative to fluorescein in 0.01 M aqueous NaOH using the well-established method described by Xu and Webb<sup>[26]</sup> and the appropriate solvent-related refractive index corrections.<sup>[30]</sup> The quadratic dependence of the fluorescence intensity on the excitation power was checked for each sample and all wavelengths.

### Acknowledgements

The authors acknowledge UEB for their financial support and China Scholarship Council (C.S.C.) for PhD funding (D.Y. and X.Z.). Dr. Mireille Blanchard-Desce (ISM, UMR 5255 CNRS, Université de Bordeaux) is gratefully acknowledged for fruitful discussions and for providing access to two-photon excited fluorescence and singlet oxygen facilities. We also thank Vincent Hugues (ISM) for his help in the photophysical measurements.

**Keywords:** dendrimers · energy transfer · fluorenyl · fluorescence · porphyrins

- [1] G. McDermott, S. M. Prince, A. A. Freer, A. M. Hawthornthwaite-Lawless, M. Z. Papiz, R. J. Cogdell, N. W. Isaacs, *Nature* **1995**, *374*, 517–521.
- [2] a) N. T. Kalyani, S. J. Dhoble, *Renewable Sustainable Energy Rev.* **2012**, *16*, 2696–2723; b) C. A. Barker, X. Zeng, S. Bettington, A. S. Batsanov, M. R. Bryce, A. Beeby, *Chem. Eur. J.* **2007**, *13*, 6710–6717.
- [3] M. G. Walter, A. B. Rudine, C. C. Wamsler, *J. Porphyrins Phthalocyanines* **2010**, *14*, 759–792.
- [4] a) X. Feng, L. Chen, Y. Dong, D. Jiang, *Chem. Commun.* **2011**, *47*, 1979–1981; b) C. Y. Lee, O. K. Farha, B. J. Hong, A. A. Sarjeant, S. T. Nguyen, J. T. Hupp, *J. Am. Chem. Soc.* **2011**, *133*, 15858–15861.
- [5] a) W.-S. Li, T. Aida, *Chem. Rev.* **2009**, *109*, 6047–6076; b) W. Maes, W. Dehaen, *Eur. J. Org. Chem.* **2009**, 4719–4752; c) B. Du, D. Fortin, P. D. Harvey, *Inorg. Chem.* **2011**, *50*, 11493–11505; d) V. Rozhkov, D. Wilson, S. Vinogradov, *Macromolecules* **2002**, *35*, 1991–1993.
- [6] a) B. Li, X. Xu, M. Sun, Y. Fu, G. Yu, Y. Liu, Z. Bo, *Macromolecules* **2006**, *39*, 456–461; b) B. Li, J. Li, Y. Fu, Z. Bo, *J. Am. Chem. Soc.* **2004**, *126*, 3430–3431.
- [7] E. M. Harth, S. Hecht, B. Helms, E. E. Malmstrom, J. M. Fréchet, C. J. Hawker, *J. Am. Chem. Soc.* **2002**, *124*, 3926–3938.
- [8] a) W. R. Dichtel, J. M. Serin, C. Edder, J. M. Fréchet, *J. Am. Chem. Soc.* **2004**, *126*, 5380–5381; b) M. A. Oar, J. M. Serin, J. M. Fréchet, *Chem. Mater.* **2006**, *18*, 3682–3692.
- [9] M. Sun, Z. J. Bo, *Polym. Sci. Part A* **2007**, *45*, 111–124.
- [10] a) M. Kozaki, K. Akita, S. Suzuki, K. Okada, *Org. Lett.* **2007**, *9*, 3315–3318; b) M. Kozaki, A. Uetomo, S. Suzuki, K. Okada, *Org. Lett.* **2008**, *10*, 4477–4480; c) A. Uetomo, M. Kozaki, S. Suzuki, K.-I. Yamanaka, O. Ito, K. Okada, *J. Am. Chem. Soc.* **2011**, *133*, 13276–13279; d) M. Kozaki, S. Morita, S. Suzuki, K. Okada, *J. Org. Chem.* **2012**, *77*, 9447–9457.
- [11] a) S. Drouet, C. Paul-Roth, G. Simonneaux, *Tetrahedron* **2009**, *65*, 2975–2981; b) S. Drouet, C. O. Paul-Roth, *Tetrahedron* **2009**, *65*, 10693–10700; c) A. Merhi, S. Drouet, N. Kerisit, C. O. Paul-Roth, *Tetrahedron* **2012**, *68*, 7901–7910; d) D. Yao, V. Hugues, M. Blanchard-Desce, O. Mongin, C. O. Paul-Roth, F. Paul, *New J. Chem.* **2015**, *39*, 7730–7733.
- [12] a) J. N. G. Pillow, M. Halim, J. M. Lupton, P. L. Burn, I. D. W. Samuel, *Macromolecules* **1999**, *32*, 5985–5993; b) M. J. Frampton, R. Beavington, J. M. Lupton, I. D. W. Samuel, P. L. Burn, *Synth. Met.* **2001**, *121*, 1671–

- 1672; c) M. J. Frampton, S. W. Magennis, J. N. G. Pillow, P. L. Burn, I. D. W. Samuel, *J. Mater. Chem.* **2003**, *13*, 235–242.
- [13] a) M. Schmittl, S. Samanta, *J. Org. Chem.* **2010**, *75*, 5911–5919; b) M. Ayabe, K. Yamashita, K. Sada, S. Shinkai, A. Ikeda, S. Sakamoto, K. Yamaguchi, *J. Org. Chem.* **2003**, *68*, 1059–1066; c) K. Sonogashira, Y. Tohda, N. Hagihara, *Tetrahedron Lett.* **1975**, *16*, 4467–4470.
- [14] Y. Zhuang, R. W. Hartmann, *Arch. Pharm. Pharm. Med. Chem.* **1999**, *332*, 25–30.
- [15] a) F. Malvoti, C. Rouxel, A. Triadon, G. Grelaud, N. Richy, O. Mongin, M. Blanchard-Desce, L. Toupet, F. I. Abdul Razak, R. Stranger, M. Samoc, X. Yang, G. Wang, A. Barlow, M. P. Cifuentes, M. G. Humphrey, F. Paul, *Organometallics* **2015**, *34*, 5418–5437; A. Triadon, M. G. Humphrey, F. Paul, unpublished results.
- [16] A. D. Adler, F. R. Longo, J. D. Finarelli, J. Goldmacher, J. Assour, L. Korsakoff, *J. Org. Chem.* **1967**, *32*, 476–476.
- [17] J. S. Lindsey, H. C. Hsu, I. C. Schreiman, *Tetrahedron Lett.* **1986**, *27*, 4969–4970.
- [18] a) S. Drouet, A. Merhi, D. Yao, M. P. Cifuentes, M. G. Humphrey, M. Wielgus, J. Olesiak-Banska, K. Matczyszyn, M. Samoc, F. Paul, C. O. Paul-Roth, *Tetrahedron* **2012**, *68*, 10351–10359; b) K. Onitsuka, H. Kitajima, M. Fujimoto, A. Iuchi, F. Takei, S. Takahashi, *Chem. Commun.* **2002**, 2576–2577.
- [19] M. Ranger, M. Leclerc, *Macromolecules* **1999**, *32*, 3306–3313.
- [20] C. Paul-Roth, G. William, J. Letessier, G. Simonneaux, *Tetrahedron Lett.* **2007**, *48*, 4317–4322.
- [21] C. Xu, W. W. Webb, *J. Opt. Soc. Am. B* **1996**, *13*, 481–491.
- [22] The dihedral angle between the phenyl rings and the macrocycle is more than 60° in TPP, see: S. J. Silvers, A. Tulinsky, *J. Am. Chem. Soc.* **1967**, *89*, 3331–3337.
- [23] a) M. Drobizhev, Y. Stepanenko, Y. Dzenis, A. Karotki, A. Rebane, P. N. Taylor, H. L. Anderson, *J. Am. Chem. Soc.* **2004**, *126*, 15352–15353; b) D. Y. Kim, T. K. Ahn, J. H. Kwon, D. Kim, T. Ikeue, N. Aratani, A. Osuka, M. Shigeiwa, S. Maeda, *J. Phys. Chem. A* **2005**, *109*, 2996–2999; c) M. Drobizhev, Y. Stepanenko, Y. Dzenis, A. Karotki, A. Rebane, P. N. Taylor, H. L. Anderson, *J. Phys. Chem. B* **2005**, *109*, 7223–7236; d) K. Ogawa, H. Hasegawa, Y. Inaba, Y. Kobuke, H. Inouye, Y. Kanemitsu, E. Kohno, T. Hirano, S.-i. Ogura, I. Okura, *J. Med. Chem.* **2006**, *49*, 2276–2283; e) S. Achelle, P. Couleaud, P. Baldeck, M.-P. Teulade-Fichou, P. Maillard, *Eur. J. Org. Chem.* **2011**, 1271–1279.
- [24] a) O. Mongin, M. Sankar, M. Charlot, Y. Mir, M. Blanchard-Desce, *Tetrahedron Lett.* **2013**, *54*, 6474–6478; b) O. Mongin, V. Hugues, M. Blanchard-Desce, A. Merhi, S. Drouet, D. Yao, C. Paul-Roth, *Chem. Phys. Lett.* **2015**, *625*, 151–156.
- [25] N. S. Makarov, M. Drobizhev, A. Rebane, *Opt. Express* **2008**, *16*, 4029–4047.
- [26] D. D. Perrin, W. L. F. Armarego, *Purification of Laboratory Chemicals*, 3rd ed., Pergamon, Oxford, **1988**.
- [27] J. D. Megiatto, Jr., R. Spencer, D. I. Schuster, *J. Mater. Chem.* **2011**, *21*, 1544–1550.
- [28] H. Tani, F. Toda, K. Matsumiya, *Bull. Chem. Soc. Jpn.* **1963**, *36*, 391–396.
- [29] C. L. Devi, K. Yesudas, N. S. Makarov, V. J. Rao, K. Bhanuprakash, J. W. Perry, *J. Mater. Chem. C* **2015**, *3*, 3730–3744.
- [30] M. H. V. Werts, N. Nerambourg, D. Pélégry, Y. Le Grand, M. Blanchard-Desce, *Photochem. Photobiol. Sci.* **2005**, *4*, 531–538.

Received: November 17, 2015

Revised: February 2, 2016

Published online on March 2, 2016